

7-1-2006

Effects of annealing conditions on ferroelectric nanomesa self-assembly

Mengjun Bai

University of Missouri, Columbia, baime@missouri.edu

Matt Poulsen

University of Nebraska-Lincoln, map@suiter.com

Stephen Ducharme

University of Nebraska, sducharme1@unl.edu

Follow this and additional works at: <http://digitalcommons.unl.edu/physicsducharme>



Part of the [Physics Commons](#)

Bai, Mengjun; Poulsen, Matt; and Ducharme, Stephen, "Effects of annealing conditions on ferroelectric nanomesa self-assembly" (2006). *Stephen Ducharme Publications*. 33.

<http://digitalcommons.unl.edu/physicsducharme/33>

This Article is brought to you for free and open access by the Research Papers in Physics and Astronomy at DigitalCommons@University of Nebraska - Lincoln. It has been accepted for inclusion in Stephen Ducharme Publications by an authorized administrator of DigitalCommons@University of Nebraska - Lincoln.

Submitted January 23, 2006; revised June 20, 2006; published July 21, 2006.

Effects of annealing conditions on ferroelectric nanomesa self-assembly

Mengjun Bai¹, Matt Poulsen, and Stephen Ducharme

Department of Physics and Astronomy, Nebraska Center for Materials and Nanoscience, University of Nebraska–Lincoln, Lincoln, NE 68588-0111, USA

¹ Present address: Department of Physics, University of Missouri, Columbia, MO 65211, USA.

Correspondence emails: baime@missouri.edu and sducharme1@unl.edu

Abstract

We report the results of studies of the effects of annealing conditions on the morphology of ferroelectric nanomesas. The nanomesa patterns were fabricated by self-assembly from continuous ultra-thin Langmuir–Blodgett films of copolymers of vinylidene fluoride and trifluoroethylene. Annealing in the paraelectric phase induced surface reorganization into disc-shaped ferroelectric nanomesas approximately 9 nm thick and 100 nm in diameter. Several factors affect the nanomesa dimensions, such as polymer composition, substrate material, deposition conditions, and annealing temperature. The height and diameter of the nanomesas both increase with increasing annealing temperature. Annealing studies in the ferroelectric–paraelectric coexistence region show that only the paraelectric phase is mobile. From this we conclude that the paraelectric phase supports a kind of plastic crystalline flow connected with dynamic disorder of the polymer conformation.

1. Introduction

Self-assembly is an effective means of producing nanoscale structures in parallel through a bottom-up approach, in contrast to a top-down approach like photolithography. A common method of self-assembly of polymers is to alternate segments with different physical properties, so-called block copolymers [1], so that periodic patterns form spontaneously during crystallization. This strategy is often not viable with polymers that have finely tuned physical properties that would be disturbed by block copolymerization. In these cases, self-assembly may be achieved through dynamical instabilities that arise in ultrathin fluid films [2]. One example of instability-driven self-assembly is the formation of ferroelectric nanomesas and nanowells [3, 4] from Langmuir–Blodgett (LB) films of the copolymers of vinylidene fluoride (VDF) and trifluoroethylene (TrFE) [5], in which plastic deformation or plastic flow play an essential role [6, 7]. Ultrathin LB films of P(VDF-TrFE) copoly-

mers are initially continuous and flat [8], but annealing in the paraelectric phase results in the spontaneous appearance of isolated ferroelectric nanomesas approximately 9 nm thick by 100 nm in diameter, with the polymer chains lying parallel to the substrate [3]. The uniform shape and flat top of the nanomesas imply that their formation involves a surface reorganization process [4, 9, 10], a kind of crystalline plastic flow [6, 7], rather than liquid flow associated with melted or glassy materials. The nanomesas have the same (110) crystal orientation [3] as the continuous LB films [5], which means the polymer chains remain in plane. The round nanomesa morphologies are very different from those of lamellar crystals, which tend to form faceted crystals in which the chains fold up and down across the thinnest dimension [11–13]. Controlling the size, shape, crystallinity and orientation of the nanomesas is important for practical device fabrication. In addition, understanding the nanomesa formation mechanism may provide useful insights into plastic flow in other polymer crystals. Here, we report the results of studies of the effect of annealing conditions on nanomesa dimensions. These results show that factors such as film composition, annealing temperature, substrate composition, and annealing time all affect the size and shape of the nanoscale structures. Furthermore, the results show that the material flow occurs only in the paraelectric phase, indicating the importance of dynamic bond disorder in the self-assembly process.

2. Experimental methods

The nanomesas were fabricated by annealing ultrathin films of ferroelectric copolymers fabricated by Langmuir–Blodgett deposition on various substrates [3]. The films consisted of random copolymers of P(VDF-TrFE) with VDF:TrFE molecular ratios of 75:25, 70:30, and 50:50, and weight-averaged molecular weights M_w (and corresponding all-trans lengths) of 178,200 amu (660 nm), 100,000 amu (370 nm) and 116,000 amu (400 nm), respectively. The continuous copolymer films were deposited by the horizontal (Schaefer) variation of the LB technique using a NIMA model 622C automated LB trough filled with ultra-pure ($>18\text{ M}\Omega\text{ cm}$) water. The LB films were deposited on substrates of electronic-grade (100) silicon wafers with a native oxide layer, or silicon wafers coated with aluminum or gold films by vacuum evaporation. Film preparation methods have been described in greater detail previously [5]. For the present studies, each LB film consisted of a single layer transferred from the water surface at a pressure of 5 mN m^{-1} . Previous studies of P(VDF-TrFE 70:30) LB films show that one nominal monolayer (ML) produced in this way averages 1.8 nm thickness [14], and we expect the other VDF copolymer compositions to have a similar thickness. To produce the nanomesas, the films were annealed in air for 1 h (unless otherwise noted), with heating and cooling rates of 1°C min^{-1} [3]. The nanomesa images were recorded by an atomic force microscope (AFM, Digital Instruments model Dimension 3100). The x-ray diffraction (XRD) data were obtained with a θ - 2θ x-ray diffractometer (Rigaku D/Max-B) with a fixed Cu anode source (wavelength = 0.154 nm).

3. Results

The nanomesa morphology is highly dependent on the annealing temperature. The annealing temperature studies were performed on a series of 1 ML LB films of P(VDF-TrFE 75:25) deposited on a silicon substrate. Each film was annealed once and then imaged with the AFM. Figure 1 shows the evolution of the film morphology as a function of annealing temperature. As the annealing temperature was increased, the film morphology changed gradually from a continuous film to a broken matrix with interstitial voids,

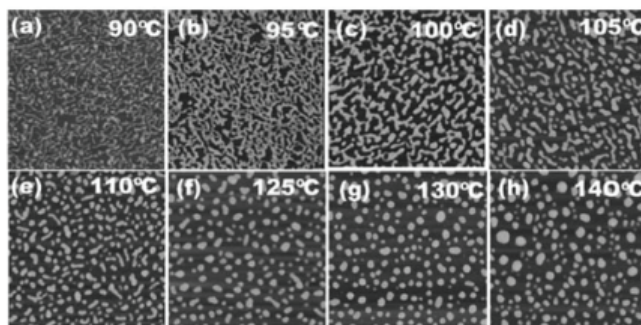


Figure 1. AFM images of 1 ML LB films of the 75:25 copolymer deposited on Si wafers show the gradual development of the morphology as the annealing temperature is increased. The images all represent film areas $2\ \mu\text{m}$ by $2\ \mu\text{m}$.

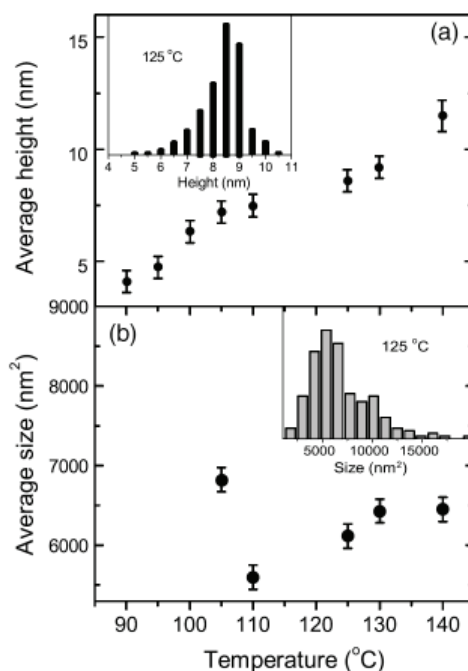


Figure 2. (a) The averaged height of the surface features from the AFM images in figure 1 shows an increasing trend with increased annealing temperature. Inset: the height distribution of the nanomesa from the image annealed at $125\ \text{°C}$. (b) The averaged area of the nanomesas from the images in figure 1 at 105 , 110 , 125 , 130 , $140\ \text{°C}$ shows a slightly increasing trend with increasing temperature for annealing temperatures above $110\ \text{°C}$, well in the paraelectric phase. Inset: the area distribution of the nanomesas from the sample annealed at $125\ \text{°C}$.

and then to isolated nanomesas. The height of the annealed structures in each image was determined by measuring the step heights on a series of line scans across the AFM image [3]. The average film height was taken from the centroid of a histogram of the step heights, like the one shown in the inset to figure 2(a), which corresponds to the film annealed at $125\ \text{°C}$. Figure 2(a) shows that the average height increases from $4.1 \pm 0.5\ \text{nm}$ to $11.5 \pm 0.5\ \text{nm}$ as the annealing temperature is increased. For the films annealed at $105\ \text{°C}$

and higher, the nanomesas were well enough separated so their average area could be determined by the image processing software supplied with the AFM, producing a nanomesa area histogram like the one shown in the inset to figure 2(b). The dependence of the average area on annealing temperature shows an abrupt decrease from the 105 °C annealing temperature to the 110 °C annealing temperature, which we attribute to the vanishing of the remaining ferroelectric phase followed by a steady increase with increasing annealing temperature. Since both the height and area of the nanomesas increased with increased annealing temperature, the nanomesa volume is not fixed by initial conditions, as it would be if each nanomesa originated from a single crystal or grain in the continuous film. Consider also that the disc shape belies the underlying atomic order of the crystal. Since the chains are oriented parallel to the substrate [3] and are much longer than the nanomesa diameter, they must fold to keep within the perimeter.

The morphology of the annealed films is more complex if the annealing temperature is within the coexistence region T_{C1} – T_{C2} corresponding to the gradual conversion from the ferroelectric to paraelectric phases, a consequence of the enthalpy difference between the two phases for a system undergoing a first-order phase transition [15]. Films annealed at temperatures below T_{C1} do not have any paraelectric component and therefore remain continuous. The lack of voids below T_{C1} also indicates that little amorphous material is originally present in the films, since the glass transition temperature is well below room temperature, –40 °C for PVDF [16]. Films annealed above T_{C2} are completely paraelectric, and therefore are free to form separated equilibrium nanomesa structures, as in figures 1(e)–(h). Annealing at temperatures within the coexistence region produced intermediate patterns, as is evident in the AFM images in figures 1(a)–(e). At lower temperatures in the coexistence region between temperatures T_{C1} and T_{C2} , where the immobile ferroelectric portion is still percolating, the mobile paraelectric polymer is trapped, leaving only isolated voids, as is evident in figures 1(a) and (b). At higher temperatures in the coexistence region, where the ferroelectric portion is no longer percolating, the images in figures 1(c) and (d) show irregular islands that are not necessarily representative of the nanomesas. This may explain why annealing at 105 °C does not completely break up the film. These observations imply that the coexistence region spans the limiting temperatures $T_{C1} \approx 90$ °C and $T_{C2} \approx 110$ °C in the 75:25 copolymer films and $T_{C1} \approx 50$ °C and $T_{C2} \approx 65$ °C in the 50:50 copolymer films [16].

We can quantify the amount of mobile polymer, and therefore the amount of paraelectric material during annealing, by measuring the fractional void area in each AFM image, which is the ratio of the area without polymer to the total image area. Figure 3 shows the dependence of the fractional void area on annealing temperature for two copolymer compositions, 75:25 and 50:50. Films held at room temperature or annealed at low temperatures do not break up at all, so they have zero void area. Films annealed in the coexistence region show some void area, but do not develop isolated mesas. We propose that this is because only part of the film is in the paraelectric phase and therefore only part of the film is mobile. (The calculated void area continues to increase above T_{C2} because the nanomesa heights are increasing and this reduces the area they take up.) This gradual change, from no void area to partial void area, and then to nanomesas, further supports the hypothesis that only the paraelectric phase flows [3]. A series of 20 AFM images, each 4 μm by 4 μm square, from 75:25 copolymer samples annealed at temperatures ranging from 90 to 140 K, was analyzed to determine the volume of polymer on the substrate. The average volume of $7.2 \pm 0.4 \times 10^3 \text{ nm}^3$ corresponds to an *average* film thickness of $1.8 \pm 0.1 \text{ nm}$, which is consistent with the average layer thickness of $1.78 \pm 0.07 \text{ nm}$ determined by ellipsometry for continuous LB films of the 70:30 copolymer [14].

The phase coexistence and refinement of crystal structure by annealing are evident in the θ – 2θ x-ray diffraction data from a 3 ML film of the 70:30 copolymer deposited on sil-

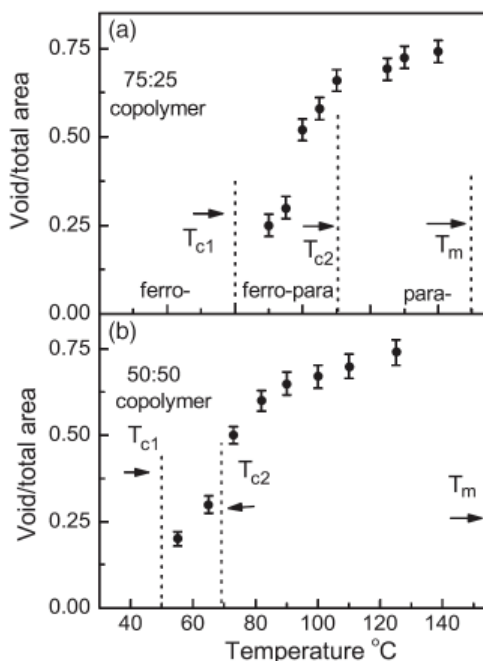


Figure 3. Plot of the void fraction, the ratio of void area to the total image area, determined from the AFM images of 1 ML LB films annealed at different temperatures: (a) for the 75:25 copolymer films; and (b) for the 50:50 copolymer films. The dashed lines labeled T_{c1} , T_{c2} and T_m represent the lower phase coexistence limit, the upper phase coexistence limit, and the melting point, respectively.

icon. The x-ray data in figure 4 show (110) diffraction peaks near 19° for the ferroelectric phase and near 18° for the paraelectric phase [17]. Figure 4 shows the diffraction data recorded at fixed temperatures during an annealing cycle during heating (figure 4(a)) and cooling (figure 4(b)). The temperature was stabilized at each step and then diffraction data were recorded for 15 min. Heating gradually converts the film from paraelectric to ferroelectric, as indicated by the appearance of a peak near $2\theta = 18^\circ$ at a temperature of approximately 90°C . At 120°C , the sample is completely paraelectric and has considerably improved crystallinity, which is retained upon cooling back to room temperature. The film was continuous before annealing, and exhibited nanomesas after annealing, so there must have been significant flow of the polymer while the film was in the crystalline paraelectric phase. It is possible that the polymer melts, flows into round islands, and then recrystallizes in a time short compared to the 15 min needed to complete one x-ray scan. In the case of melting polyethylene lamellae, such melting and recrystallization has been observed, but only if the film temperature is raised above the bulk melting point [18, 19]. The melting points of these copolymers are all above 140°C , however, and the copolymer LB films show no melting at lower temperatures [20]. Further, we find that LB films of PVDF, which melts directly from the ferroelectric phase without passing through a paraelectric phase [21], and polyethylene, which is not ferroelectric at all, do not develop voids or nanomesas when annealed just below their melting points.

Additional evidence that the nanomesas represent the equilibrium endpoint of a slow reorganization process comes from observations of the nanomesa patterns as a function of annealing time. The nanomesa or nanowell patterns formed on LB films of 1–4 ML are well formed when annealed at 125°C or higher for 30 min or longer. Re-annealing a film at the same temperature did not change the overall morphology if the first anneal was an

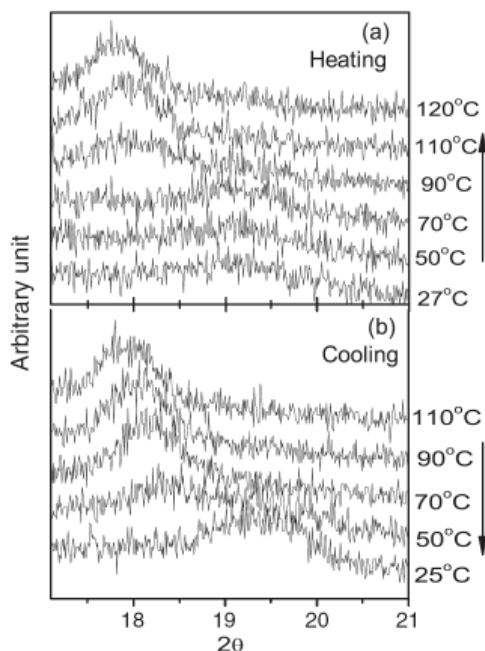


Figure 4. The x-ray diffraction data recorded from a fresh 3 ML LB film of the 70:30 copolymer deposited on a Si wafer, as the sample was heated, the film annealed for 1 h at 125 °C, and then cooled.

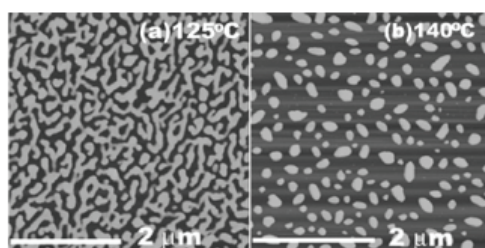


Figure 5. AFM images of a 2 ML 75:25 copolymer LB film (a) annealed for 1 h at 125 °C and (b) re-annealed for 1 h at 140 °C. The two images were recorded from different regions of the sample about 2 μm apart, but represent typical morphologies on the sample.

hour or more, up to 24 h in our studies. Briefly annealing the films with thicknesses of 1 ML and 2 ML by putting them directly into an oven preheated to 125 °C for only 10 min and then removing them to cool in air showed irregular isolated nanomesas for 1 ML samples and percolating nanomesas for 2 ML samples (see figure 5(a)), indicating that the film reorganization time is of the order of 10 min. The percolated or elongated nanomesas obtained by annealing the continuous film at 125 °C were transformed to rounded nanomesas with increased area and height when they were re-annealed at 140 °C (see figure 5(b)). The change in nanomesa volume after a second annealing further supports the hypothesis that nanomesa volume is primarily a function of annealing conditions.

The composition of the polymer also affects the nanomesa morphology. The nanomesas formed from the 70:30 and 75:25 copolymers had similar dimensions, while those formed from the 50:50 copolymer were much smaller. Since the 75:30 and 50:50 had sim-

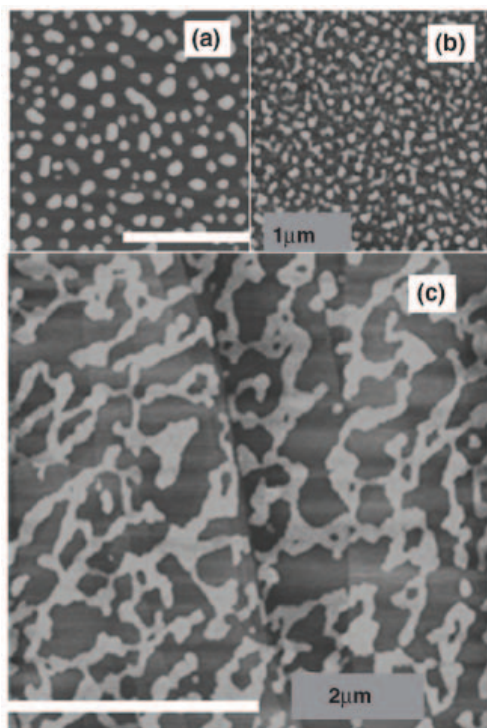


Figure 6. AFM images of the structures formed from 1 ML LB films of the 75:25 copolymer deposited on three different surfaces and annealed at 125 °C for 1 h. (a) Nanomesas from a 1 ML film deposited on the half of a silicon wafer coated with an aluminum film 10 nm thick. (b) Nanomesas on the same silicon wafer but on the half without an aluminum film. (c) Morphology of a 2 ML film deposited on highly oriented pyrolytic graphite.

ilar molecular weights, and the 70:30 molecular weight was about 75% higher, it does not seem that the nanomesa dimensions are sensitive to molecular weight. There does seem to be a correlation with the upper critical temperature T_{C2} , which is much smaller in the case of the 50:50 copolymer compared to the values for the 70:30 and 75:25 copolymers.

The substrate material also affects the nanomesa morphology, as might be expected from differences in interface adhesion energies [13, 22]. This is evident in the AFM images (figures 6(a), (b)) of a 1 ML film made on a Si wafer which had one half of its top surface coated with 10 nm of aluminum, and was then annealed at 125 °C. The nanomesas are much smaller on the aluminum-coated side, indicating that the interface energy of the polymer is greater there. Films deposited on a glass slide coated with gold and platinum films also produced smaller nanomesas. The roughness of the substrate also affects nanomesa roughness. The rms roughness of the nanomesas was 0.3 nm on the plain silicon side and 0.9 nm on the aluminum side, due largely to the rougher aluminum surface. However, a smooth surface is not essential to form such nanomesa patterns. Figure 6(c) shows an AFM image of a 2 ML 75:25 copolymer film deposited on a highly oriented pyrolytic graphite (HOPG) substrate and annealed at 125 °C. The steps in the graphite surface appear to affect the nanomesa morphology.

4. Discussion

These results show the nanomesa morphology depends on the annealing conditions, LB film thickness, polymer composition, substrate material, and substrate morphology. The results also imply that the polymer flows and forms nanostructures in its paraelectric phase, but not in the ferroelectric phase, and that the film remains crystalline during flow. There are two key observations supporting this hypothesis. First, the nanomesas are flat with steep sides, not rounded, as one would expect for the shape of a liquid drop. Sec-

ond, the *in situ* x-ray diffraction data show that the LB films remain crystalline at temperatures sufficiently high to produce nanomesas, and that there is significant material flow even in the phase coexistence region. Furthermore, the nanomesas exhibit the same essential physical properties of the continuous LB films [5], specifically, (110) crystal orientation, all-trans ferroelectric crystal structure and polarization hysteresis at room temperature, and a reversible ferroelectric–paraelectric phase transition [3]. Melting results in lamellae with very different morphologies [23]. Therefore, we conclude that the films remain crystalline during annealing and that nanomesa formation is the result of plastic crystalline flow. We first consider how flow might occur in the crystalline paraelectric phase, then how it might transform continuous LB films as thin as 1.8 nm into arrays of mesa-shaped structures.

To understand the mechanism of plastic crystalline flow, we need to consider the difference in structure between the ferroelectric and paraelectric phases. The ferroelectric phase consists of linear polymer chains with all-trans conformation, in which the carbon atoms lie in a plane and the chains are arranged in a quasi-hexagonal close-packed structure [16]. The (110) *d*-spacing of 0.45 nm in the ferroelectric phase leaves little free volume in the crystal. The paraelectric phase consists of linear polymer chains with an alternating trans-gauche conformation, where the gauche bonds have random helicity, resulting in a hexagonal packing with a (110) spacing of 0.51 nm and therefore a considerable amount of free volume [24]. It has been proposed that this random trans-gauche structure is not static, but rapidly fluctuating on a picosecond time scale [25, 26]. Such fluctuations, along with the increased volume in the paraelectric phase, should allow plastic flow of the polymer, where chains can shift position through local density fluctuations, without having to cross each other. This would also permit flow both parallel and perpendicular to the polymer chains, though the flow rates in these directions would likely be quite different. This plastic flow may also enable chain folding and unfolding, allowing the nanomesas to reshape themselves.

The nanomesa morphology is distinctly different from the morphology of lamellar crystals, which are generally in the form of thin faceted plates, in which the chains are perpendicular to the substrate, folding back and forth along the shortest dimension [11]. The critical thickness of lamellar crystals is determined by folding statistics and is dependent on temperature [27–29]. Substrate interactions [22] or other mechanical confinement [12] can influence the lamellar morphology, in which free surface tension was hindered by substrate confinement. Solvent-crystallized PVDF and its copolymers generally form spherulites of needle-like crystals, in which the chain folding is again along the shortest dimension [30]. Faceted lamellar crystals were obtained from the thicker LB films after melting and recrystallization, in which the chains are perpendicular to canted facets, and are no longer parallel to the substrate [23]. The nanomesas, on the other hand, have their chains parallel to the substrate and upper surfaces parallel to the substrate.

The round shape of the nanomesas, besides being quite different morphologies from that typically observed in lamellar crystals, belies the underlying crystal structure. Since the chains lie predominantly parallel to the substrate, one would expect an elongated, faceted structure. To produce round structures, the surface energies must be large enough to induce sufficient chain folding at the perimeter, and possibly in the interior as well [4]. Figure 7 shows a possible construction that resembles lamellar crystals in the sense that there is coherent folding, but quite different in the sense that the polymer chains are perpendicular to the shortest dimension. Chain folding [27, 28] is a key feature in the crystallization of lamellar crystals of polyethylene, PVDF [18], polyethylene oxide [31], and other crystalline polymers [11], in which the chain segments are usually along the shortest dimension. Interactions with the substrate may serve to keep the chains in plane. A similar effect was observed in 20 nm thick films of drawn polyethylene, in which the films showed lamellar folding and contoured perimeters, but with the chains oriented parallel to



Figure 7. Top view of a hypothetical nanomesa showing several chain-folding structures that may be present. Some of the chains may extend beyond the perimeter and return elsewhere, leaving amorphous loops similar to those found on the faces of lamellar crystals [11, 12].

the surfaces due to the extreme draw ratio and the consequent larger surface tension [12]. Inside the nanomesa, the chains could fold back and forth during annealing, perhaps involving chain exit and reentry and/or molecule pinning; the fold positions are guided by the perimeter surface energy to follow a curve, as shown in figure 7. Future work on the nanomesas should include high-resolution studies of nanomesa structure.

5. Summary

The reorganization and self-assembly of VDF copolymer films made by LB deposition depends on several factors, such as annealing temperature, polymer composition, substrate material and roughness, and deposition conditions. The formation mechanism seems to involve plastic crystalline flow in the paraelectric phase, while the mesa shape and dimensions seem to be governed by surface energies. The results suggest that this type of plastic crystalline flow may be found in other crystalline polymers that have a similar dynamic trans-gauche phase. These fabrication methods could be used to produce a variety of nanostructured transducers for, for example, high-density nonvolatile random-access memories, acoustic transducer arrays, and infrared imaging arrays and templates.

Acknowledgments

We thank S-H. Liou, and L. P. Yue for assistance with the AFM, D. S. Devreddy for molecular weight measurements, and J. Li and V. M. Fridkin for helpful discussions. The ferroelectric copolymers used for this work were provided by V. M. Fridkin of the Institute of Crystallography, Moscow, and by Mitch Thompson of Measurement Specialties, Inc. This work was supported by the National Science Foundation and the Nebraska Research Initiative.

References

- [1] Bates F S and Fredrickson G H 1990 Block copolymer thermodynamics: theory and experiment *Annu. Rev. Phys. Chem.* **41** 525–57
- [2] Flitton J C and King JR 2004 Surface-tension-driven dewetting of Newtonian and power-law fluids *J. Eng. Math.* **50** 241–66
- [3] Bai M and Ducharme S 2004 Ferroelectric nanomesa formation from polymer Langmuir–Blodgett films *Appl. Phys. Lett.* **85** 3528–30

- [4] Li J, Luo Y, Bai M, and Ducharme S 2005 Nanomesa and nanowell formation in Langmuir–Blodgett polyvinylidene fluoride trifluoroethylene copolymer films *Appl. Phys. Lett.* **87** 213116
- [5] Ducharme S, Palto S P, and Fridkin V M 2002 Ferroelectric polymer Langmuir–Blodgett films *Ferroelectric and Dielectric Thin Films* ed. HS Nalwa (San Diego, CA: Academic) pp. 545–91
- [6] Séguéla R 2002 Dislocation approach to the plastic deformation of semicrystalline polymers: kinetic aspects for polyethylene and polypropylene *J. Polym. Sci. B* **40** 593–601
- [7] Flores A, Calleja F J B, and Asano T 2001 Creep behavior and elastic properties of annealed cold-drawn poly(ethylene terephthalate): the role of the smectic structure as a precursor of crystallization *J. Appl. Phys.* **90** 6606–10
- [8] Bune A V, Fridkin V M, Ducharme S, Blinov L M, Palto S P, Sorokin A V, Yudin S G, and Zlatkin A 1998 Two-dimensional ferroelectric films *Nature* **391** 874–7
- [9] Reiter G, Castelein G, and Sommer J-U 2001 Liquidlike morphological transformations in monolamellar polymer crystals *Phys. Rev. Lett.* **86** 5918–21
- [10] Wong G C L, Commandeur J, Fischer H, and de Jeu W H 1996 Orientational wetting in hybrid liquid crystalline block copolymers *Phys. Rev. Lett.* **77** 5221
- [11] Geil P H 1963 *Polymer Single Crystals* (New York: Interscience)
- [12] Eng L M, Jandt K D, Fuchs H, and Petermann J 1994 Scanning force microscopy of the crystalline/amorphous interface of ultradrawn poly(ethylene) *Appl. Phys. A* **59** 145–50
- [13] Reiter G and Sommer J U 1998 Crystallization of adsorbed polymer monolayers *Phys. Rev. Lett.* **80** 3771–4
- [14] Bai M, Sorokin A V, Thompson D W, Poulsen M, Ducharme S, Herzinger C M, Palto S, Fridkin V M, Yudin S G, Savchenko V E, and Gribova L K 2004 Determination of the optical dispersion in ferroelectric vinylidene fluoride (70%)/trifluoroethylene (30%) copolymer Langmuir–Blodgett films *J. Appl. Phys.* **95** 3372–7
- [15] Lines M E and Glass A M 1977 *Principles and Applications of Ferroelectrics and Related Materials* (Oxford: Clarendon)
- [16] Tashiro K 1995 Crystal structure and phase transition of PVDF and related copolymers *Ferroelectric Polymers* ed. H S Nalwa (New York: Dekker) pp 63–181
- [17] Choi J, Borca C N, Dowben P A, Bune A, Poulsen M, Pebley S, Adenwalla S, Ducharme S, Robertson L, Fridkin V M, Palto S P, Petukhova N N, and Yudin S G 2000 Phase transition in the surface structure in copolymer films of vinylidene fluoride (70%) with trifluoroethylene (30%) *Phys. Rev. B* **61** 5760–70
- [18] Wang T T, Herbert J M, and Glass A M (ed) 1988 *The Applications of Ferroelectric Polymers* (Glasgow/New York: Blackie/Chapman and Hall)
- [19] Nalwa H S (ed) 1995 *Ferroelectric Polymers* (New York: Dekker)
- [20] Poulsen M, Adenwalla S, Ducharme S, Fridkin V M, Palto S P, Petukhova N N, and Yudin S G 2000 Use of an external electric field to convert the paraelectric phase to the ferroelectric phase in ultra-thin copolymer films of P(VDF-TrFE) *Ferroelectric Thin Films IX (Boston, Nov.–Dec.) (Proceedings of the Materials Research Society* vol. 655) ed. P C McIntyre, S R Gilbert, Y Miyasaka, R W Schwartz, and D Wouters (Pittsburgh, PA: Materials Research Society) pp. CC10.4.1–6
- [21] Furukawa T 1989 Ferroelectric properties of vinylidene fluoride copolymers *Phase Transit.* **18** 143–211
- [22] Frank C W, Rao V, Despotopoulou M M, Pease R F W, Hinsberg W D, Miller R D, and Rabolt J F 1996 Structure in thin and ultrathin spin-cast polymer films *Science* **273** 912–15
- [23] Bai M, Poulsen M, Sorokin A V, Ducharme S, and Fridkin V M 2001 Morphology, annealing, and melting of ferroelectric Langmuir–Blodgett films of vinylidene fluoride (70%) trifluoroethylene (30%) copolymer *Conf. on Electroactive Polymers and Their Applications as Actuators, Sensors, and Artificial Muscles (Boston, Nov. 2001) (Proceedings of the Materials Research Society* vol. 698) ed. Q Zhang, E Fukada, Y Bar-Cohen and S Bauer (Pittsburgh, PA: Materials Research Society) pp. EE2.8.2–.8.7
- [24] Bellet-Amalric E and Legrand J F 1998 Crystalline structures and phase transition of the ferroelectric P(VDF-TrFE)copolymers, a neutron diffraction study *Eur. Phys. J. B* **3** 225–36
- [25] Dvey-Aharon H, Sluckin T J, and Taylor P L 1980 Kink propagation as a model for poling poly(vinylidene fluoride) *Phys. Rev. B* **21** 3700–7
- [26] Stock-Schweyer M, Meurer B, and Weill G 1994 High pressure effect on molecular motions in the paraelectric phase of a vinylidene fluoride and trifluoroethylene copolymer (70/30) studied by n.m.r *Polymer* **35** 2072–7
- [27] Lauritzen J I and Hoffman J D 1960 *J. Res. Natl Bur. Stand.* **64** 73
- [28] Sadler D M 1987 New explanation for chain folding in polymers *Nature* **326** 174–7
- [29] Doye J P K and Frenkel D 1998 Mechanism of thickness determination in polymer crystals *Phys. Rev. Lett.* **81** 2160
- [30] Lovinger A J 1983 Ferroelectric polymers *Science* **220** 1115–21
- [31] Reiter G A and Sommer J U 2000 Polymer crystallization in quasi-two dimensions. I. Experimental results *J. Chem. Phys.* **112** 4376–83